EXPERIMENTAL AND NUMERICAL STUDY OF TURBULENT JET SHEAR LAYER INTERACTING WITH A FREE SURFACE

Nimesh Virani
Department of Mechanical, Automotive and Materials Engineering
University of Windsor
401 Sunset Avenue, Windsor, Ontario, N9B 3P4, Canada
viranin@uwindsor.ca

Vesselina Roussinova
Department of Mechanical, Automotive and Materials Engineering
University of Windsor
401 Sunset Avenue, Windsor, Ontario, N9B 3P4, Canada
vtr@uwindsor.ca

Ram Balachandar
Department of Civil and Environmental Engineering
University of Windsor
401 Sunset Avenue, Windsor, Ontario, N9B 3P4, Canada
rambala@uwindsor.ca

ABSTRACT

This study focuses on the interactions of a circular three-dimensional turbulent jet interacting with a free surface. This type of jet is commonly referred to as a surface jet. Volumetric three-dimensional (3D) three-component (3C) measurements are performed using 3D Particle Tracking Velocimetry (PTV). To compensate for some of the limitations of experimental measurement techniques near a free surface, a complementary high-fidelity Large Eddy Simulation (LES) is also performed. Free surface (air-water interface) is modelled using the Volume of Fluid (VOF) technique. Experimental and numerical results are compared for numerical model validation. The study provides interesting insights into the jet-free surface interaction region. The suitability of volumetric measurement technique for this experiment was validated using a Laser Doppler Velocimetry (LDV) system in our previous work (Virani et al. 2022).

The study is performed with a relatively high jet Reynolds number (*Re*) of 20,300 based on the jet exit centerline velocity (U_j = 2.9 m/s) and the jet diameter (d = 7 mm). The jet is submerged at a depth $h = 3d$ from the free surface. The current study aims to provide a detailed analysis of the evolving turbulent flow structures, including the formation of vortical structures, entrainment, and surface currents within the confined jet and their influence on the free surface.

INTRODUCTION

Surface jets are formed when a high momentum fluid exiting from a nozzle or source interacts with a free surface. The interplay between this jet and the surrounding medium holds significant importance in various domains, including the study of river and coastal dynamics, the optimization of industrial processes (i.e. release of hot water from a thermal power plant in a nearby water body), and the dispersion of pollutants among others. Surface jets exhibit unique characteristics because of their proximity to the free surface, introducing complexities and interactions that differ from those seen in a submerged free jet that are void from any boundary effects. Figure 1 shows the schematic diagram of a surface jet and highlights all the main parameters involved in characterizing it. Here, U_c is local jet centerline velocity and U_m is local jet maximum velocity. Depending on the submergence ratio and Reynolds number, surface jet development and its effect on the free surfaces varies.

Contrary to the turbulent jet/free surface interaction, the flow characteristics of turbulent free jet have been the subject of many investigations and as a result, very well understood (Hussain and Zedan 1978; Hussein et al. 1994; Gohil et al. 2014; Mistry et al. 2016). The earliest experimental work on surface jets was conducted by Evans (1955), which was limited to observing the presence of surface waves and surface currents and no turbulent flow structures were studied. Over a period of time, various researchers attempted to study different parameters affecting the behaviour of surface jets such as Reynolds number, Froude number, submergence depth and nozzle shape (Anthony and Willmarth 1992; Madnia and Bernal 1994; Walker et al. 1995; Sankar et al. 2009; Tay et al. 2017). Anthony and Willmarth (1992) investigated the mean velocity field and the Reynolds stresses of a circular turbulent surface jet. The study was conducted using a three-component Laser Doppler Velocimetry (LDV) technique. They found that the turbulent fluctuations in the direction perpendicular to the free surface were diminished, while those aligned with the surface were intensified. Additionally, they observed the presence of an outward flow, moving away from the jet axis, within a thin layer situated near the free surface, which is called ‘surface currents’.

Herein, a key focus is put on understanding the mechanism driving the surface currents. Their formation and propagation were studied by previous researchers; however, there is a void in the complete understanding of turbulence within the surface current layers (Walker 1997). It was observed that turbulent mixing significantly reduces within the surface current because of turbulence redistribution from

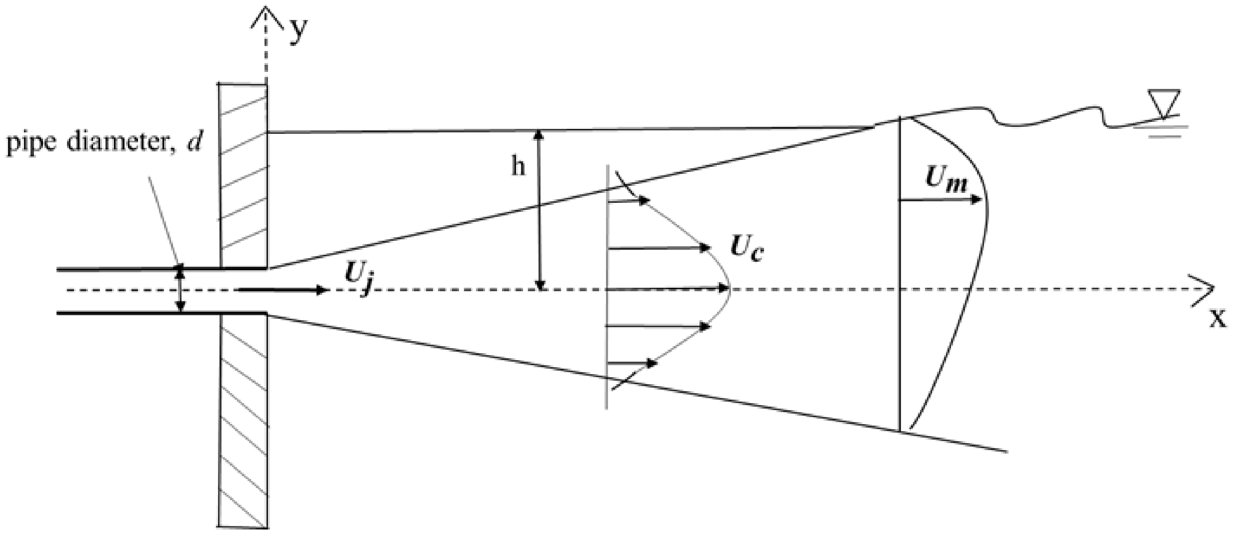

Figure 1. Surface jet schematic describing all the important parameters which defines a surface jet

the vertical velocity component (perpendicular to the free surface) to the other two velocity components (Tian et al. 2012; Wen et al. 2014). Though the vertical velocity gets diminished by the presence of the free surface, this turbulence redistribution mechanism remains not completely understood. This also hints that to study this problem in its entirety, point measurement techniques like LDV and planar PIV measurement are not sufficient due to the inherent three-dimensional nature of this problem. However, a surface jet three-dimensional dataset is missing in the literature and hence, we have implemented Volumetric PIV measurements along with scale-resolving LES simulation to resolve the flow field in space and time domains.

METHODOLOGY

Experimental

Experiments are performed in the Jet Experimental Facility at the University of Windsor. The jet is generated from a pipe, with a diameter d = 7 mm and located at h/d = 3 from the free surface. This effectively results in a Froude number (Fr) of ~ 6.4. The jet is released into a quiescent water channel section with a cross-section of 43d × 43d in y and z directions respectively. The water channel is made from a transparent Plexiglas material, which enables optical access for velocity measurement. For this study, x, y and z coordinates correlate to streamwise, transverse and spanwise directions, respectively. The instantaneous and corresponding fluctuating velocities in x, y and z directions are denoted by u, v, w, and u', v', and w', respectively. Also, the associated mean velocities are defined by U, V, and W. The channel measurement section is 200d long in the streamwise direction. The jet is fed by an overhead water tank and the tank is maintained at a constant level by a continuous water supply from a reservoir using a pump. A sharp edge weir downstream of the jet is used, to maintain the constant height of free surface from the jet centerline during the experiment. More details on the jet facility and the experimental setup can be found in our earlier work (Virani et al. 2022).

The volumetric PTV system (V3V) consists of three cameras mounted on a custom-designed triangular-shaped stand, a dual pulsed Nd: YAG laser (200 mJ/pulse) and a synchronizer for connecting all these components with the computer. The flow is illuminated by a laser cone generated from 25 mm and 50 mm cylindrical lenses staggered at the laser opening. The flow is seeded by 60 µm polyamide particles. All 3 cameras have a CCD array with 8 million pixels and 3320 × 2496 resolution, and they are equipped with 50-mm lenses with the aperture setting of f#8. The camera mounting frame is levelled and adjusted to ensure that it is parallel with the walls of the channel using an alignment laser. Laser pulses are straddled at 200 µs and the measurement was performed at 5 Hz. A total of 3000 images are captured and analyzed with a final measuring region of 20d × 14d × 7d. Details of volumetric calibration, data processing and post-processing are described in (Virani et al. 2022).

Numerical

The numerical simulation domain is designed to mimic the experimental jet facility described above. The inlet section of the jet which consists of a 10d long pipe, is also included in the simulation domain. This makes sure that not only the mean flow but also turbulence quantities are mapped correctly at the jet exit plane into the channel. At the inlet boundary of the pipe nozzle, a constant mass flow rate of 0.1 kg/s and turbulence intensity of 5% are applied. The turbulence level at the nozzle inlet is selected based on a systematic study performed by (Virani et al. 2021). All the other sides of the domain (except pipe walls and domain side

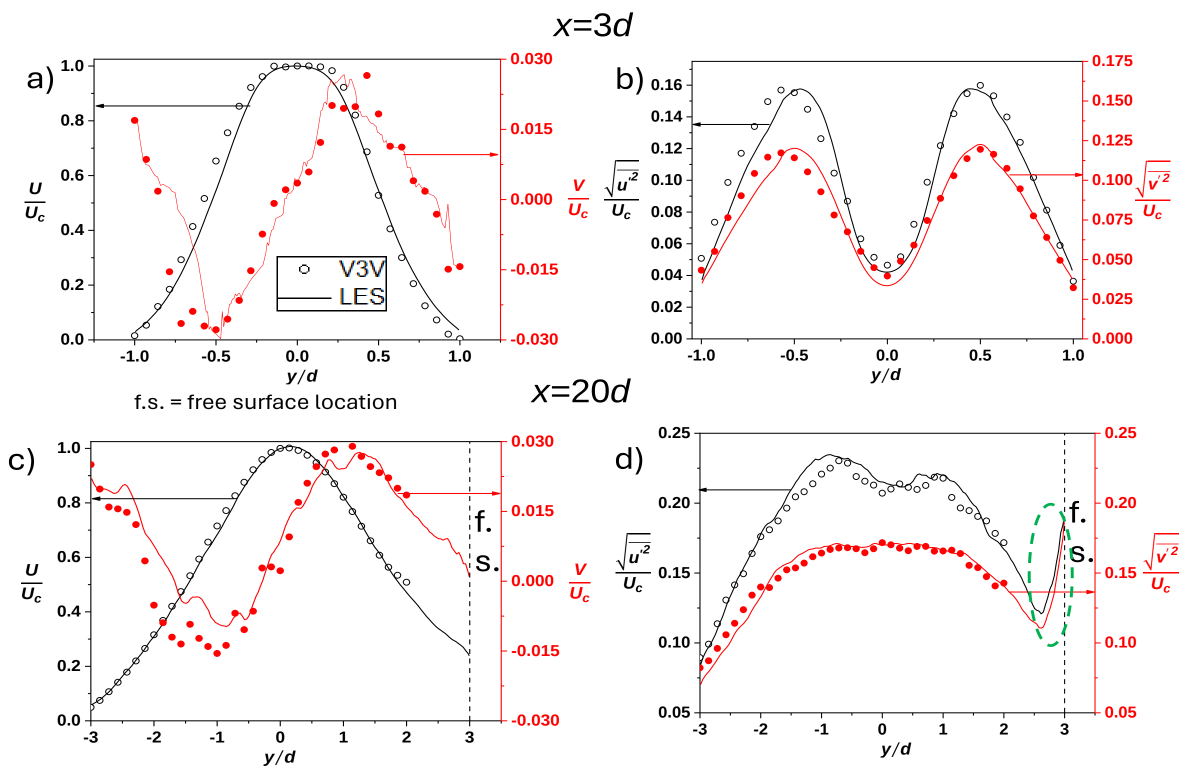

Figure 2. Experimental and numerical data comparison in the near field and far field of the jet. The circle symbol denotes V3V data, and the line represents LES data. The dotted vertical line describes the position of the free surface location.

walls) are treated as constant pressure outlets which mimic the open-to-atmosphere condition present in the channel and facilitate reverse flow at the boundaries. Sharp edge weir present in the experimental domain is reproduced in the numerical domain as well.

Commercial code STAR-CCM+ 13.06.012 is used for this study which is a finite volume method-based code. High-fidelity scale resolving LES simulation is performed in both water and air domains. While the air-water interface is resolved by the Volume of Fluid (VOF) method. For closing the subgrid-scale part (SGS) of LES the Dynamic Smagorinsky model is used as it was found suitable to study free jets by (Salkhordeh and Kimber 2019). The suitability of VOF and LES models to resolve free surface flows with high fidelity is discussed in detail by (Jesudhas 2016; Sarkar and Savory 2021). For VOF, the hydrostatic pressure of water based on the initial height of water is used as an initial condition in the water domain. No numerical wave damping is used since the simulation domain width matches the channel size used for experiments. Time marching is performed using a fully implicit second-order scheme with the time step size of 5.0×10^{-5} s, which is estimated based on the smallest turbulent time scale present in the flow. In total simulation is run for 19.35 seconds of physical time and data samples are collected (for calculating mean and turbulence quantities) over 13.6 seconds at the sampling rate of 20 KHz. This equals the time averaging over 56 flow-throughh cycles based on the jet exit velocity and for a 100d-long domain.
The simulation grid is designed based on guidelines provided by Celik et al. (2005) and it was customized to resolve turbulent length scales up to the Taylor microscales.

Precursor RANS simulations are run iteratively to find the correct distribution of Taylor microscales used for the mesh design. The final mesh has 67 million cells. Further details for the mesh designing procedure used for simulating a jet flow and free surface flow are provided in (Jesudhas 2016; Virani et al. 2019).

RESULTS

For volumetric PTV, mean and turbulence quantities are calculated on a regular grid (equally spaced) by spatial binning and ensemble averaging over 3000 data sets. The procedure to reach time-average data points in the measurement volume from uncorrelated snapshot is described in detail in our previous work (Virani et al. 2022). Since the V3V data is limited up to 20*d* in the streamwise direction of jet, it is used for validation of numerical data. For further analysis in the downstream direction from $20d < x < 100d$ LES data is used. However, rigorous validation of surface jet mean and turbulence quantities is presented in Figure 2. Also, due to the severe laser light reflections coming from the moving free surface, experimental data is limited up to one diameter of jet inside the water domain. Free surface perturbations created by the interaction between the turbulent jet and free surface saturate the camera pixels and hampers capturing any meaningful images. However, numerical simulation does not face this limitation and that's one of the main reasons to include LES simulation in this work.

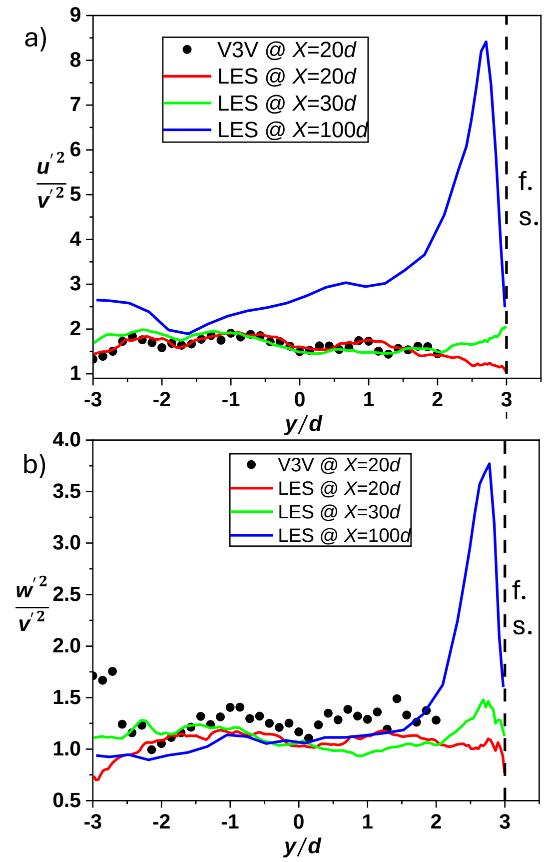

Figure 3. Ratios between square of turbulence fluctuations in the directions parallel to the free surface and perpendicular to the free surface at different axial locations of the jet

Some preliminary results are presented in Figures 2 (a – d). Figure 2 (a) and (b) shows the comparison between experimental and numerical data close to the jet exit at x/d = 3. Mean and turbulence quantities in the jet radial direction are compared. For this location, jet's growth is limited as it's in the beginning face of development. Also, the free surface is at a considerable distance from the jet and hence mean and turbulence profiles here resemble a free jet. This can be seen by the symmetry between the bottom part of the jet (negative y/d locations) and the part which is closer to the free surface (+ y/d locations).

Figure 2 (a) shows the streamwise mean velocity (on the left axis) and transverse mean velocity (right axis), as well as Figure 2 (b), shows the RMS of streamwise turbulence fluctuations (on the left axis) and RMS of transverse turbulence fluctuation (on the right axis). All the quantities are normalized by the local centreline velocity, U_c and the radial position is normalized by the jet diameter, *d*. Peak turbulence level and mean velocity profile in the potential core and shear layer regions show excellent agreement between the two datasets.

Similarly, Figure 2 (c) and (d) show the same quantities at the jet's farther downstream location of x/d = 20. At this location, the jet has grown and started interacting with the free surface. Here, the experimental dataset is limited up to a radial location of y/d = 2 due to the experimental limitation discussed earlier. The vertical dashed line indicates the location of the undisturbed free surface in these graphs. For the numerical dataset, all the quantities presented here are distinguished from the air domain by using the volume fraction of water ≥0.5 as a cut-off value. In other words, a volume fraction of 0.5 is used as a boundary between water and air fluids which is a common practice adopted in similar previous studies (Nasif et al. 2016; Jesudhas et al. 2016). This is important to make sure that the data used here only belongs to the water region. This comparison between V3V and LES data suggests that even though, experimental data is not available close to the free surface, everywhere else, both the datasets show strong agreement.

The presence of interaction between the jet and the free surface can be confirmed by the elevated levels of streamwise and transverse turbulence fluctuations very close to the free surface. It is highlighted in Figure 2 (d) by a green dotted line circle. This behaviour of turbulence fluctuations near the free surface was also observed by Anthony and Willmarth (1992) and Walker et al. (1995). Although this is a starting point of the jet's engagement with the free surface, this is not a complete engagement, as shown later here. Overall, this comparison between the experimental V3V dataset and the LES numerical results validates the suitability of the numerical dataset for further investigation of surface jet flow.

To further investigate the redistribution of turbulence kinetic energy caused by the presence of the free surface, ratios of turbulence fluctuations are investigated at different axial locations. Previous researchers Tian et al. (2012) and Tay et al. (2017) studied the jet's interaction with a dynamic boundary like free surface at different axial locations. Their finding suggests that turbulence quantities continuously vary along the streamwise direction in surface jets, and this can be seen in Figure 3 (a) and (b) as well.

Figure 3 (a) shows the ratio between the square of streamwise turbulence fluctuations and transverse turbulence fluctuations at three different axial locations: x/d = 20, x/d = 30 and x/d = 100 along the radial direction. Similarly, Figure 3(b) shows the ratio between the square of spanwise and transverse turbulence fluctuations. Here, the reasoning for choosing these specific locations is as follows: x/d = 20 is the farthest axial location where experimental data is available and Figure 1(d) suggests that the free surface has started affecting mean and turbulence quantities at this location. x/d = 30 is the first location where both the ratios seem to start changing close to the free surface compared to the other part of the jet away from the free surface. x/d = 100 is the farthest point where the numerical data is available, and the jet is completely attached to the free surface at this location. In both figures, experimental data for x/d = 20 location is included for comparison.

These ratios highlight the difference in the strength of turbulence fluctuations in the directions parallel (*x, and z*) and perpendicular (*y*) to the free surface in the proximity of the free surface. This was also observed by Tay et al. (2017) for two different submergence ratios of the jet. However, they only had access to planar data in the vertical plane, so they did not compare the spanwise turbulence fluctuations against transverse. Not only, do Figures 3 (a) and (b) suggest that turbulence energy redistribution occurs from the component perpendicular to the free surface to the other two components (parallel to it) but also that the redistribution is not symmetric. At the farthest location, x/d = 100, streamwise turbulence fluctuation is up to ~8 times larger

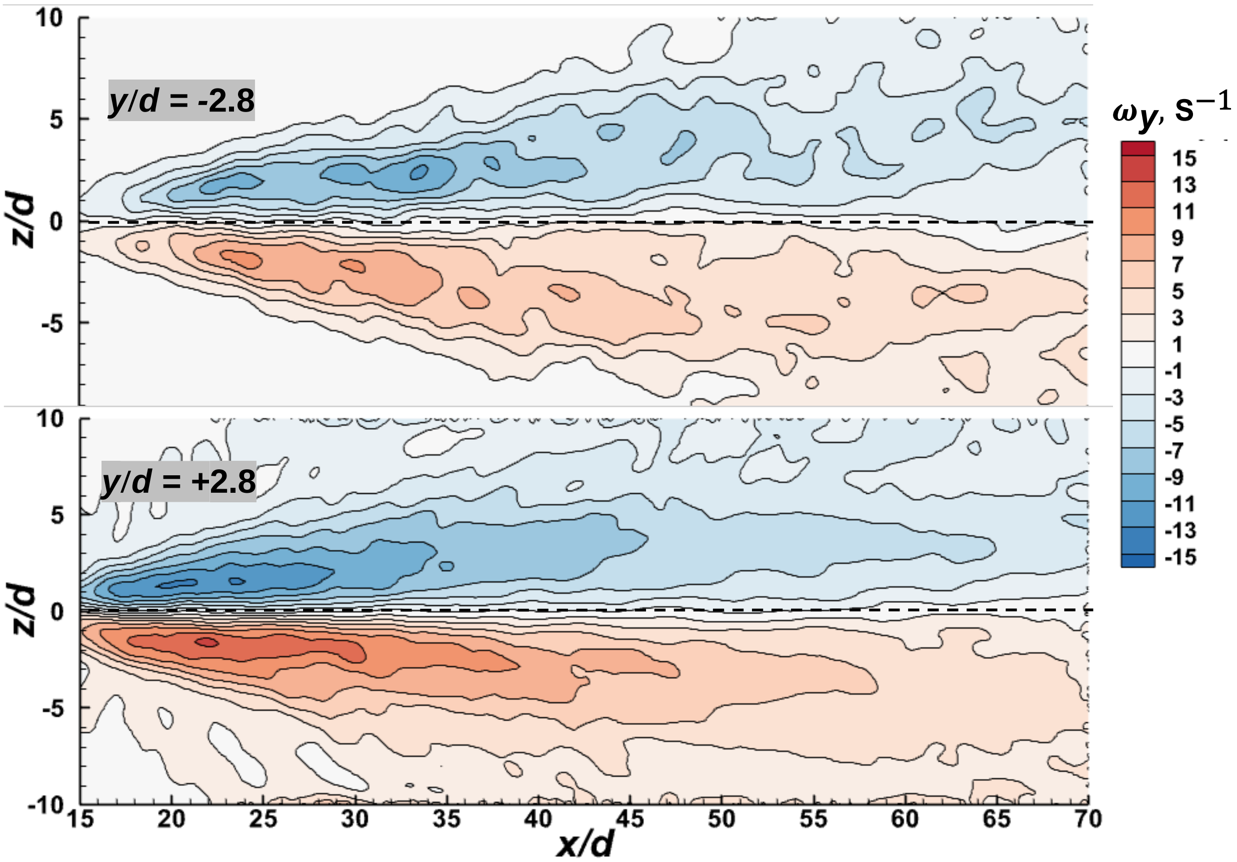

Figure 4. Comparison of mean y-vorticity on a plane parallel to the free surface and located at two different radial positions: closer and away from the free surface.

than the transverse component, while spanwise fluctuations are ~4 times larger at the same location. This behaviour for surface jets where the streamwise component gains a larger share from the damping of the transverse component than the spanwise component was also observed by Walker et al. (1995). They attributed this to the fact that turbulence kinetic energy is produced in the streamwise velocity fluctuations and is then transferred to the fluctuations in the other velocity components. Additionally, each ratio increases in magnitude as the jet grows farther downstream These ratios steadily increase as jet interacts with the free surface between x/d = 30 and x/d = 100 and other locations are not shown here for brevity.

Figure 3 (a) and (b) show that away from the free surface turbulence is reasonably isotropic, and an anisotropic turbulence region is created by the presence of a free surface closer to it. Similar results were found by Walker et al. (1995). They investigated surface jets with two different Reynolds numbers and Froude numbers with significantly different values of these governing numbers. Their high Froude number case is similar to the one investigated here. The presence of anisotropy in turbulence fluctuations near the free surface alters the mixing characteristics of the jet as mixing can be directly correlated to the level of turbulence fluctuations present in the flow (Brown and Roshko 1974; Browand 1986). This also indicates the practical significance of studying high Reynolds number surface jet flows.

Interaction between a free surface and a vorticity field was discussed by many previous researchers in the context of surface currents created by it (Anthony and Willmarth 1992; Walker et al. 1995; Walker 1997). Walker (1997) stated a conjecture regarding origin of the surface current that the surface current is related to the interaction of tangential vorticity with a free surface. A theoretical framework was also provided in this study to support the hypothesis. However, due to the lack of a three-dimensional dataset, it was not proven.

Figure 4 shows the mean y-vorticity component (ω_y – perpendicular to the free surface) in a plane parallel to the free surface at two different radial locations. The dotted centerline indicates the centerline of the jet. Figure 4 indicates that the magnitude of y-vorticity is enhanced by the free surface in a plane closer to it compared to the plane away from it. Vorticity filed in a surface jet was also studied using PIV data by (Essel et al. 2020). However, due to the deeper submergence of the jet, they did not find a significant influence of the free surface on vorticity field in the plane parallel to the free surface. Figure 4 not only shows the larger vorticity magnitude near free surface but also hints at broader growth of the jet compared to the away from the free surface. This could affect the jet mixing characteristics to a great extent similar to the change in turbulence fluctuations discussed earlier.

CONCLUSIONS

Fundamental study of interaction between a flexible boundary like a free surface and a shear layer like the one generated by a turbulent jet is very crucial for many practical applications. The complex and highly three-dimensional nature of this problem requires volumetric experimental/numerical techniques to study it. Due to the additional complexity introduced by the air-water interface, experimental techniques lag in providing information near the free surface. Hence, the volumetric PTV technique and scale-resolving Large Eddy Simulation are implemented in this work to study the surface jet problem. Preliminary results highlight some interesting findings which can be briefly summarised as follows.

- Volumetric data set obtained using V3V techniques and LES simulations have a good match and proves the validity of using the LES + VOF approach to study surface jet
- Turbulence fluctuations redistribute near the free surface from the component perpendicular to the free surface to the one parallel to it.
- This redistribution is not equally divided between the streamwise and spanwise components. Streamwise component gains significantly higher amount of energy than the spanwise.
- Vorticity field and jet growth width are affected by the presence of the free surface in a plane close to it.

REFERENCES

Anthony, D.G., and Willmarth, W. W.,1992, "Turbulence Measurements in a Round Jet Beneath a Free Surface", *Journal of Fluid Mechanics,* Vol. 243, pp. 699–720.

Browand, F.K., 1986, "The structure of the turbulent mixing layer", *Phys Nonlinear Phenom*, Vol. 18, pp. 135–148.

Brown, G.L., Roshko, A., 1974, "On density effects and large structure in turbulent mixing layers". *Journal of Fluid Mechanics*, Vol. 64, pp. 775–816.

Celik I. B., Cehreli Z. N., and Yavuz I., 2005, "Index of Resolution Quality for Large Eddy Simulations", *Journal of Fluids Engineering,* Vol. 127, pp. 949–958

Essel, E. E., Roussinova, V., Balachandar, R., 2020, " Free surface effects on spanwise turbulent structure in the far-field of submerged jets", *Physics of Fluids,* Vol. 32 pp-35108.

Evans J. T., 1955, "Pneumatic and Similar Breakwaters", *Proceedings of the Royal Society of London*, Vol. 231, pp. 457–466.

Gohil, T. B., Saha, A. K., and Muralidhar, K., 2014, "Large Eddy Simulation of a Free Circular Jet", *Journal of Fluids Engineering*, Vol. 136, pp. 051205.

Hussain, A. K. M. F., Zedan, M. F., 1978, "Effects of the Initial Condition on the Axisymmetric Free Shear Layer: Effects of the Initial Momentum Thickness", *Physics of Fluids,* Vol. 21, p p. 1100–1112.

Hussein, H. J., Capp, S. P., and George, W. K., 1994, "Velocity Measurements in a High-Reynolds-number, momentum-conserving, Axisymmetric, Turbulent Jet", *Journal of Fluid Mechanics*, Vol. 258, pp. 31–75.

Jesudhas, V., 2016, "Modeling of Free-Surface Flows with Air Entrainment" Electron Theses Diss

Jesudhas, V., Roussinova, V., Balachandar, R., Barron, R., 2016, "Submerged Hydraulic Jump Study Using DES", *Journal of Hydraulic Engineering*, 04016091-1-04016091–11.

Madnia, C. K., Bernal, L. P., 1994, "Interaction of a Turbulent Round Jet with the Free Surface", *Journal of Fluid Mechanics*, Vol. 261, pp. 305–332.

Mistry, D., Philip, J., Dawson, J. R., and Marusic, I., 2016, "Entrainment at Multi-scales Across the Turbulent/non-turbulent Interface in an Axisymmetric Jet", Journal of Fluid Mechanics. Vol. 802, pp. 690–725.

Nasif, G., Balachandar, R., Barronm R.M., 2016, " Mean characteristics of fluid structures in shallow-wake flows", *International Journal of Multiphase Flow*, Vol. 82, pp-74–85.

Salkhordeh, S., Kimber M.L., 2019, "Full-Field Dependence on Inlet Modeling of Non-Isothermal Turbulent Jets Using Validated Large Eddy Simulations", *Journal of Fluids Engineering*, Vol- 141.

Sankar, G., Balachandar, R., and Carriveau, R., 2009, "Characteristics of a Three-Dimensional Square Jet in the Vicinity of a Free Surface", *Journal of Hydraulic Engineering*, Vol. 135, pp. 989–994.

Sarkar, D., Savory, E., 2021, "Numerical Modeling of Freestream Turbulence Decay Using Different Commercial Computational Fluid Dynamics Codes", Journal of Fluids Engineering, Vol. 143.

Tay, G. F. K., Rahman, M. S., and Tachie, M. F., 2017, "Characteristics of a Horizontal Square Jet Interacting with the Free Surface", *Physical Review Fluids*, Vol. 2, pp. 064607.

Tian, J., Roussinova, V., Balachandar, R., 2012, "Characteristics of a Jet in the Vicinity of a Free Surface", Journal of Fluids Engineering, Vol. 134, pp- 031204.

Virani, N., Roussinova, V., and Balachandar, R., 2022, "Three-Dimensional Turbulent Jet Study Using Volumetric Particle Tracking Velocimetry", *Proceedings, 12th International Symposium on Turbulence and Shear Flow Phenomena*, Osaka, Japan, July 19-22, 2022.

Virani, N., Roussinova, V., and Balachandar, R, 2021, "Influence of Nozzle Inlet Initial Turbulence Level on the Development of an Axisymmetric Turbulent Jet", *Proceedings, 29th Annual Conference of the Computational Fluid Dynamics Society of Canada*, Online, July 27-29, 2021.

Virani, N., Roussinova, V., and Balachandar, R., 2019, "Resolution Quality Indices for Large Eddy Simulation in Modelling a Turbulent Free Jet", *Proceedings, 4th Thermal and Fluids Engineering Conference,* pp. 1835-1845.

Walker, D. T., 1997, "On the Origin of the 'Surface Current' in Turbulent Free-surface Flows", *Journal of Fluid Mechanics*, Vol. 339, pp. 275–285.

Walker, D. T., Chen, C. Y., and Willmarth, W. W., 1995, "Turbulent Structure in Free-surface Jet Flows", *Journal of Fluid Mechanics*, Vol. 291, pp. 223–261.

Wen, Q., Kim, H. D., Liu, Y. Z., and Kim, K. C., 2014, "Dynamic Structures of a Submerged Jet Interacting with a Free Surface", *Experimental Thermal and Fluid Science*, Vol. 57, pp. 396–406.